Melting, Freezing, and Channeling Phenomena in Ice Counterwashers

Thermal phenomena are associated with the operation of ice counterwashers, a major component for the separation of ice and brine in freeze crystallization processes. Melting, freezing, and channeling in the upper leg of the counterwasher occur because of the temperature difference between the wash water and the ice and have important effects on the operation of the device. In the present study, these phenomena are modeled and analyzed and their scaling laws derived. Ice and wash water temperature distributions as well as variations in porosity and wash water flow rate due to melting and freezing in the ice plug are computed and plotted. The effect of channeling on counterwasher operation is studied and formulated in terms of the channel dimensions and ice plug properties. Growth rates of channels due to melting by the wash water are calculated. Results indicate that warm wash water and slow motion of the ice plug cause rapid channel growth and may be deleterious to counterwasher operation. Best conditions for recovery from channeling are obtained with wash water temperature close to freezing and high plug velocity.

GERSHON GROSSMAN

Faculty of Mechanical Engineering
Technion—Israel Institute of Technology
Haifa, Israel

SCOPE

Ice counterwashers are a major component in the freeze crystallization process for water purification, where pure water is extracted from the raw water in the form of ice (Brian, 1968). In this process, the raw water is cooled in a crystallizer by one of several available methods to form a mixture of small ice crystals and concentrated brine. The mixture is pumped into a counterwasher, where the ice crystals are separated from the brine and washed. The ice is then melted to give fresh water.

The counterwasher normally consists of a vertical column with a screen in the middle part of its wall, as shown schematically in Figure 1. The slurry of ice crystals and brine enters the column at the bottom. The ice particles consolidate to form a porous plug; the brine flows up through the lower leg of this plug and out through the screen. The drag of the brine on the plug causes the latter to move up against the friction on the walls and the restraining force at the top. A small amount of fresh wash water (no more than a few percent of the total freshwater produced) is introduced into the column at the top, flows down through the upper leg of the plug, and out through the screen. A well-defined interface exists between the fresh wash water and the brine, known as the brine crown. At steady state, the brine crown position relative to the column is fixed. Washing is achieved as the plug moves through the brine crown, where the brine adhering to the crystals is displaced by wash water. The washed ice is scraped mechanically at the top.

Early investigations of separation methods for the freezing process have shown the counterwasher to be the most effective and perhaps the only acceptable device for separating the ice crystals from the brine (Brian, 1968; Barduhn, 1967). A number of studies, both theoretical and experimental, has been conducted on the operation of counterwashers. The early types used were flotation columns, where the brine was drained from the bottom and the ice plug moved up by its own buoyancy (Bosworth et al., 1959). This device, which had very limited throughput rates, was modified into a gravity counterwasher (Hahn et al., 1964) (also known as drained top) which is essentially the column described in Figure 1. Despite the limited background theory (Mixon, 1964; Hahn, 1965), gravity counterwashers have been operated successfully by several groups, both in the laboratory and on pilot plant scale (Hahn et al., 1964; Wiegandt, 1960; Consie et al., 1968; Sherwood et al., 1969), at throughput rates up to 1.25kg/s-m^2 of ice. A more fundamental understanding of the scaling laws and operating characteristics of the counterwasher was gained through a theoretical analysis of the flow and pressure distributions in the ice plug by Shwartz and Probstein (1968) which was later extended by Barak and Dagan (1970) and Kemp (1973). This led to the development of the pressurized counterwasher (Probstein and Shwartz, 1971), which is an advanced version of the gravity column shown in Figure 1. In this device (also known as flooded counterwasher), the wash water saturates the upper leg above the brine crown and is forced into the top of the column under pressure, thus keeping the brine crown low and allowing for a smaller column with higher throughput rates. A laboratory study using a 0.05 m diameter column with polyethylene particles (Shwartz and Probstein, 1969) confirmed the results of the analysis. Two pressurized counterwashers have been designed and operated on a laboratory scale (Grossman, 1972), as part of a 10m^3/day freeze desalting system. Ice throughput rates as high as 7.5kg/s-m^2 have been achieved.

Several phenomena are associated with the operation of ice counterwashers which result from the interaction between the cold ice and the slightly warmer wash water in the upper leg. Some of these phenomena may cause serious difficulties in the operation of the counterwasher. The ice slurry is formed in the crystallizer in equilibrium with the brine. The ice thus enters the column at a temperature lower than the freezing point of fresh water by an amount corresponding to the freezing point depression at the brine salinity. The temperature of the wash water entering the column from the melter is slightly higher than the freezing point (typically by 1° to 2°C). There is hence a temperature difference between the wash water and the ice which results in melting of some ice and freezing of some wash water in the upper leg, until equilibrium is reached between the two. The melting and freezing are

associated with changes in plug porosity. Also, some of the wash water introduced into the column at the top freezes before it can reach the brine crown and be effective in washing.

Another phenomenon associated with the temperature difference between wash water and ice is channeling, which greatly hampers the operation of the counterwasher. Channels start from cracks or gouges which occasionally appear in the upper leg owing to various reasons, for example, mechanical stresses in the plug. When a channel occurs, most of the wash water is diverted into it, leaving little or no wash water flowing through the bed, since the channel is the path of least resistance. This results in reduced washing efficiency and lowering of the pressure in the upper leg, which in turn causes the brine crown to rise. Small channels usually disappear as the plug moves up and is scraped at the top. However, the fact that the wash water is warmer than the ice is extremely harmful. The wash water flowing down the channel melts the ice around it and makes the channel grow both in width and in depth, which in most cases prevents it from recovering and makes the situation progressively worse.

The purpose of the present work has been to study the phenomena of melting, freezing, and channeling in ice counterwashers and see how best to deal with their effects on operation. An analysis of the melting and freezing in the upper leg is presented. Channeling phenomena and their causes and effects on operation are described, and a model for the growth and recovery of channels is developed. Experimental observations on these phenomena were made in a laboratory study of pressurized ice counterwashers described elsewhere (Grossman, 1972).

CONCLUSIONS AND SIGNIFICANCE

The melting and freezing phenomena in the upper leg of ice counterwashers have been analyzed. Variations in porosity and wash water flow rate as well as ice and wash water temperature distributions were computed and plotted (see Figure 3). The following important results were obtained:

1. In most of the upper leg, the ice and wash water are in thermal equilibrium at the freezing temperature T_o. A thin melting zone exists at the top and a thin freezing zone at the bottom (thickness δ_w and δ_i, respectively), both of the order of particle diameter.

2. Changes in plug porosity are small, of order γ_i [Equation (7)] or γ_w [Equation (19)]. The minimum porosity occurs in the equilibrium zone.

3. The wash water flow rate is at a maximum in the equilibrium zone and reaches a minimum at the brine crown. In order to have a sufficient amount of wash water at the brine crown, a larger quantity has to be introduced at the top to account for freezing inside the plug. A minimum of this quantity is required which corresponds to zero wash water loss, given by Equation (31).

Channeling phenomena in the upper leg were discussed. The damaging effect of a channel on the operation of the counterwasher is determined by two parameters: the channel depth relative to the total upper leg length and the flow resistance ratio β, given by Equation (37), which determines how much of the wash water is diverted from the bed into the channel.

The wash water flow rate and temperature distributions in the channel were computed [Equations (54) and (56)]. The flow rate variations are a direct function of variations in channel area. The characteristic length for temperature variation increases with the flow rate and decreases with the heat transfer coefficient [Equation (56]. In many typical cases, the wash water looses little of its thermal energy as it flows down the channel. It transfers the remainder of the energy to the ice at the bottom of the channel.

The growth rate of channels due to melting by the wash water was studied, and the following results were obtained:

1. The sideways growth rate of the channel [Equation (57)] is relatively slow, of order γ_w, and is proportional to the heat transfer coefficient U' Equation (47). It is independent of channel flow rate.

2. The growth rate of the channel in depth is faster than sideways, due to much higher heat transfer and melting in a packed bed than in a channel flow. However, this growth rate is opposed by the upward motion of the plug. The net growth rate [Equation (61)] is proportional to γ_w and to the ratio of downward wash water velocity at the bottom of the channel to the upward plug velocity.

3. In a steadily growing channel, the initial shape as it opened is soon forgotten, and the channel grows at a fairly constant cross section (Figure 6).

4. The best way to stop channel growth is to bring the wash water temperature as close as possible to the freezing point. Increasing the plug velocity helps too, if it is not associated with a comparable increase in wash water velocity in the channel.

The present analysis and the above conclusions provide important guidelines on the conditions necessary for an efficient and continuous operation of ice counterwashers.

MELTING AND FREEZING IN THE UPPER LEG

Consider an element of the ice plug in the upper leg of the counterwasher above the brine crown, as shown in Figure 2. The element has a cross-section area of unity and height L. We assume the upper leg to be saturated with wash water, as in a pressurized (flooded) counterwasher and the flow of wash water through the element to be one dimensional (axial).* The temperature distribution shown along the element describes qualitatively the melting and freezing process. The wash water enters the top of the column at temperature T_{wo}, higher than the freezing temperature T_o. As it flows through the upper part of the bed, the wash water melts some ice and cools down to T_o. The ice, moving up, emerges from the bottom of the element at temperature T_{io} lower than T_o. It absorbs some heat from the wash water and warms up to T_o, while some of the wash water freezes. The wash water cannot be cooled below T_o without freezing; hence its unfrozen portion comes out at the bottom of the element at T_o. Similarly, the unmelted ice comes out at the top at T_o. The

* In reality, the flow in the vicinity of the brine crown has a considerable radial component. Far enough above the brine crown, however, the flow is practically one dimensional (Shwartz and Probstein, 1968; Kemp, 1973).

melting and freezing always take place over a very short distance from the top and bottom, as will be shown later. Hence, an equilibrium zone exists in the middle part of the element between ice and wash water, where both are at the freezing temperature T_o and no heat is transferred from one to the other. The melting and freezing are associated with a change in porosity which decreases at the bottom of the element, as some wash water freezes into the plug, and increases at the top, where some ice is melted.

To calculate the changes in temperature, porosity, and wash water flow in the element, we will analyze the melting and the freezing separately, then match the two solutions in the equilibrium zone. Consider first a control volume of thickness dz at the bottom of the element, where freezing takes place. Here the wash water is at constant temperature T_o, and the ice temperature T_i varies. It is assumed that as freezing occurs the porosity of the ice is reduced, but the dimensions of the plug remain unchanged. The following four equations govern the steady state process:

(a) Continuity of wash water:

$$\frac{\partial}{\partial z}(\rho_w \epsilon v)dz = -\dot{m}dz \tag{1}$$

(b) Continuity of ice:

$$\frac{\partial}{\partial z}[\rho_i(1-\epsilon)w]dz = -\dot{m}dz \tag{2}$$

(c) Energy balance*

$$\frac{\partial}{\partial z}(\rho_w \epsilon v \lambda)dz = \frac{\partial}{\partial z}[\rho_i(1-\epsilon)wc_i(T_i - T_o)]dz \tag{3}$$

(d) Heat transfer

$$-\dot{m}[\lambda + c_i(T_o - T_i)]dz = Udz(T_o - T_i) \tag{4}$$

The four unknowns in these equations are ϵ, v, T_i, and $\dot{m}$. The boundary conditions are

$$\text{at} \quad z = 0; \quad \epsilon = \epsilon_o; \quad T_i = T_{io}; \quad v = v_o \tag{5}$$

where ϵ_o and T_{io} are the porosity and temperature of the ice plug emerging from the brine crown, both given, and v_o is the flow velocity of wash water leaving the element at the bottom. v_o is not known a priori. Its value depends on the amount of wash water introduced into the column at the top, plus the contribution from the melted ice and less the portion which freezes. v_o will therefore be treated as a parameter and will be calculated when the present solution is matched with the one for the melting at the top.

Before we proceed with the solution, let us define a dimensionless ice temperature

$$\tau_i = \frac{T_o - T_i}{T_o - T_{io}} \tag{6}$$

and a relative ice heat capacity parameter

$$\gamma_i = \frac{c_i(T_o - T_{io})}{\lambda} \tag{7}$$

We note that $\gamma_i << 1$. It would be convenient to use in the solution instead of the actual velocities the superficial velocities of wash water and ice, V and W, respectively, which are defined as follows:

$$V = \epsilon v \tag{8}$$

$$W = (1-\epsilon)w \tag{9}$$

* In this calculation, the reference energy level was chosen such that ice at the freezing point T_o has zero energy. Water at T_o, therefore, has energy λ.

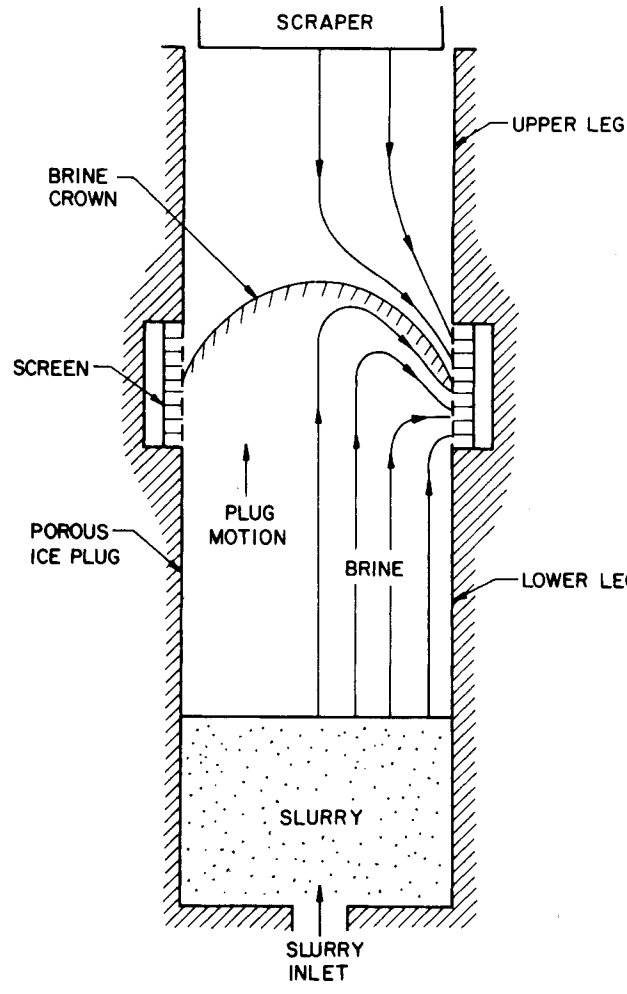

Fig. 1. Schematic representation of counterwasher.

By eliminating $\dot{m}$ between Equations (1) and (2) and integrating the resulting equation using the boundary conditions (5), we obtain a relation between the porosity and wash water superficial velocity:

$$V - V_o = \frac{\rho_i}{\rho_w} w(\epsilon_o - \epsilon) \tag{10}$$

Combining Equations (1), (2), and (3) to eliminate v and $\dot{m}$, and using the definitions (6) and (7), we get a differential relation between the temperature τ_i and the porosity, which can be integrated using the boundary conditions (5) to give

$$\frac{1-\epsilon}{1-\epsilon_o} = \frac{1+\gamma_i}{1+\gamma_i\tau_i} \tag{11}$$

Substituting $\dot{m}$ from (4) and $(1-\epsilon)$ from (11) in (2), we find

$$\rho_i(1-\epsilon_o)w(1+\gamma_i)\frac{\partial}{\partial z}\left[\frac{1}{1+\gamma_i\tau_i}\right] = \frac{U}{c_i}\frac{\gamma_i\tau_i}{1+\gamma_i\tau_i} \tag{12}$$

Assuming U = const., we can integrate (12) and obtain

$$\tau_i = \frac{e^{-z/[\delta_i(1+\gamma_i)]}}{1+\gamma_i[1-e^{-z/[\delta_i(1+\gamma_i)]}]} \tag{13}$$

where

$$\delta_i = \frac{\rho_i c_i(1-\epsilon_o)w}{U} = \frac{\rho_i c_i W_o}{U} \tag{14}$$

We now substitute (13) in (11)

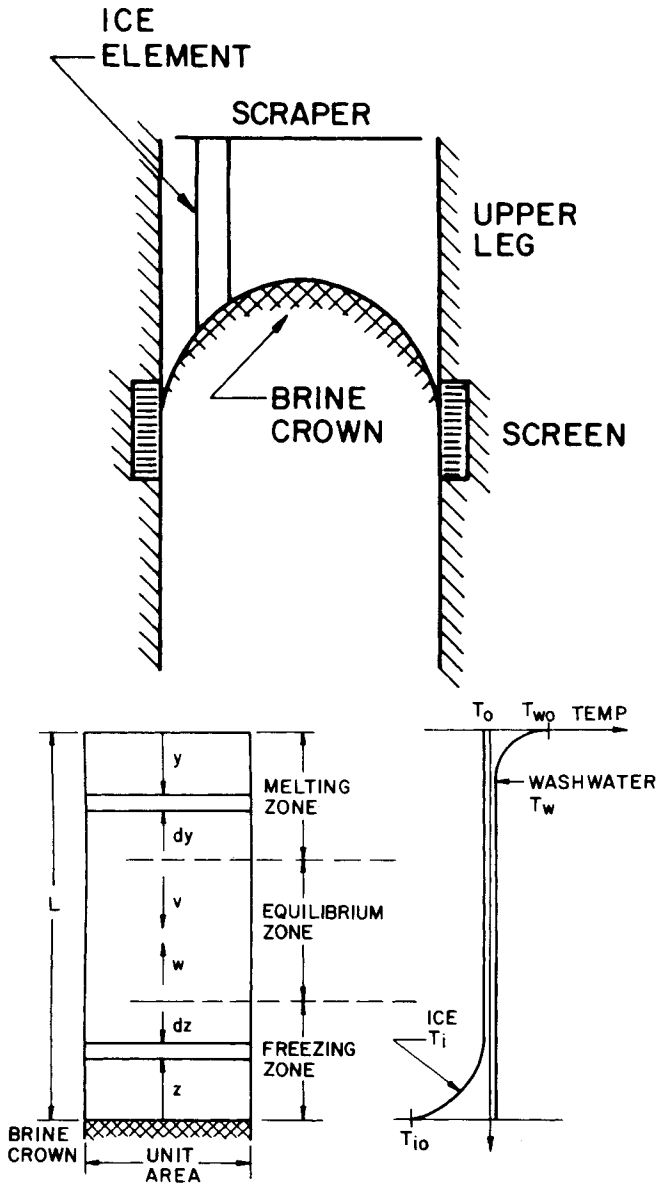

Fig. 2. Melting and freezing zones and coordinates in upper leg element.

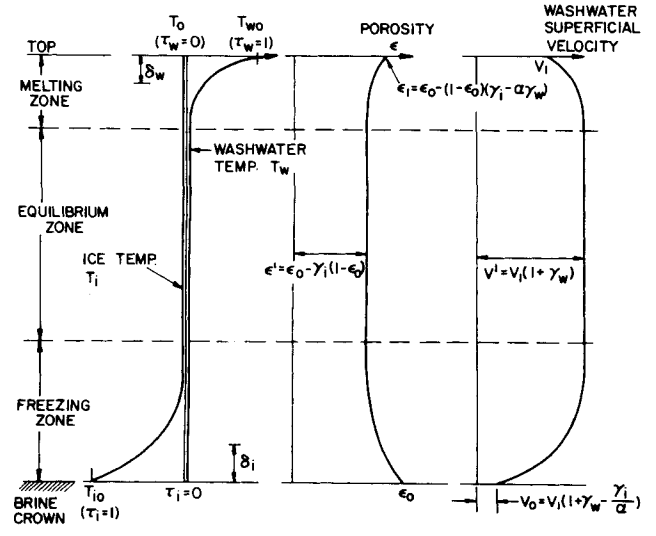

Fig. 3. Temperature, porosity, and wash water velocity distributions in upper leg.

$$\epsilon_0 - \epsilon = \gamma_i(1-\epsilon_0)\,[1 - e^{-z/[\delta_i(1+\gamma_i)]}] \qquad (15)$$

and substitute (15) in (10):

$$\frac{V - V_o}{V_o} = \frac{\rho_i W_o}{\rho_w V_o}\,\gamma_i\,[1 - e^{-z/[\delta_i(1+\gamma_i)]}] \qquad (16)$$

where V_o and W_o are the superficial velocities of the wash water and ice, respectively, at $z = 0$. Equations (13), (15), and (16) describe the variation with distance z above the brine crown of the ice temperature, the porosity, and the wash water superficial velocity, which is directly proportional to its flow rate. Equations (1) and (11) provide convenient relations between these three quantities. δ_i as given by (14) is the characteristic length over which the variations take place. Note that the variation in porosity is of order γ_i, compared to a variation of order unity in the dimensionless ice temperature τ_i. The variation in superficial wash water velocity V is given in terms of V_o, which is still to be determined by matching of this solution with the one in the melting zone.

Consider now another control volume of thickness dy at the top of the element where melting takes place. Here the ice is at constant temperature T_o, and the wash water temperature T_w varies. The analysis is very similar to the one in the freezing zone. The equations for the porosity, wash water flow rate, and wash water temperature are identical to Equations (1) through (4) with z replaced by y, $-\dot{m}$ by $+m$, $(T_o - T_i)$ by $(T_w - T_o)$, and c_i by c_w. The boundary conditions for the three unknowns are

$$\text{at}\quad y = 0 \quad \epsilon = \epsilon_1; \quad T_w = T_{wo} \quad v = v_1 \qquad (17)$$

where T_{wo} and v_1 are the temperature and the flow velocity of the wash water introduced into the column at the top, both given, and ϵ_1 is the porosity of the ice plug as it reaches the top. ϵ_1 is not known a priori and is treated as a parameter in the solution. It will be calculated later in terms of the original porosity ϵ_o, when the present solution is matched with the one in the freezing zone. We define a dimensionless wash water temperature

$$\tau_w = \frac{T_w - T_o}{T_{wo} - T_o} \qquad (18)$$

and a relative wash water heat capacity parameter

$$\gamma_w = \frac{c_w(T_{wo} - T_o)}{\lambda} \qquad (19)$$

Solving the equations as before, we get the following results:

$$\tau_w = \frac{e^{-y/[\delta_w(1+\gamma_w)]}}{1 + \gamma_w\,[1 - e^{-y/[\delta_w(1+\gamma_w)]}]} \qquad (20)$$

$$\frac{V - V_1}{V_1} = \gamma_w\,[1 - e^{-y/[\delta_w(1+\gamma_w)]}] \qquad (21)$$

$$\epsilon_1 - \epsilon = \gamma_w(1-\epsilon_1)\,\frac{\rho_w V_1}{\rho_i W_1}\,[1 - e^{-y/[\delta_w(1+\gamma_w)]}] \qquad (22)$$

where

$$\delta_w = \frac{\rho_w c_w V_1}{U} \qquad (23)$$

Here, as before, $\gamma_w << 1$. δ_w, the characteristic length of the variation, depends on the ratio between the heat contained in the wash water to the one transferred to the ice. Variations in wash water velocity are of order γ_w, as compared to temperature variations of order unity. The porosity is given in terms of ϵ_1, which is still to be determined. Note that

$$V - V_1 = \frac{\rho_i}{\rho_w} w(\epsilon - \epsilon_1) \tag{24}$$

Now, having obtained the solutions in the melting and freezing zones, in terms of the parameters V_o and V_1, we can match the two in the equilibrium zone. Setting $z \to \infty$ in Equations (13), (15), (16), and $y \to \infty$ in (20), (21), (22), we obtain in the equilibrium zone

$$\tau_i = \tau_w = 0 \qquad \text{(hence} \quad T_i = T_w = T_o\text{)}$$

$$\epsilon' = \epsilon_o - \gamma_i(1 - \epsilon_o) = \epsilon_1 - \gamma_w\alpha(1 - \epsilon_o) \tag{25}$$

$$V' = V_1(1 + \gamma_w) = V_o + V_1\frac{\gamma_i}{\alpha} \tag{26}$$

where ϵ' and V' are the porosity and the wash water superficial velocity in the equilibrium zone, respectively, and α is a wash water fraction defined by

$$\alpha = \frac{\rho_w V_1}{\rho_i W_o} \tag{27}$$

which represents the fraction of ice produced which is introduced back into the column as wash water. Normally, $\alpha << 1$. We can now obtain the values of ϵ_1 and V_o:

$$\epsilon_o - \epsilon_1 = (1 - \epsilon_o)(\gamma_i - \alpha\gamma_w) \tag{28}$$

$$\frac{V_o}{V_1} = 1 + \gamma_w - \frac{\gamma_i}{\alpha} \tag{29}$$

The results of this analysis are summarized in Figure 3, which shows the distributions of the ice and wash water temperatures, the porosity, and the wash water superficial velocity along the upper leg element. We notice that the minimum porosity in the plug occurs in the equilibrium zone. The change in porosity over the freezing zone is of order γ_i and in the melting zone of order γ_w, both relatively small compared to the original porosity. Note, however, that the magnitude of γ_i depends on the concentration of the brine entering the column. With a 1% salt concentration in the brine (as in treating brackish water), a 7% concentration (as in treating seawater), or 23% (as in eutectic freezing), the values of γ_i are approximately 0.004, 0.026, and 0.130, respectively. These lead to different values of the minimum upper leg porosity which is reduced quite considerably (compared to the original porosity) in the case of highly concentrated brine. This may be significant in determining the feasibility of operating a wash column with fresh wash water in eutectic freezing.

The wash water superficial velocity increases owing to melting from a value V_1 at the top to a maximum in the equilibrium zone, then decreases in the freezing zone and may become quite small at the bottom. The wash water loss α_o (which is the unrecovered part of the wash water, leaving the counterwasher through the brine screen, expressed as a fraction of the total fresh water produced) can be expressed in terms of the wash water fraction α by

$$\alpha_o = \frac{\rho_w V_o}{\rho_i W_o} = (1 + \gamma_w)\alpha - \gamma_i \tag{30}$$

We note that for given values of γ_i and γ_w there is a minimum value of α below which all the wash water introduced into the column at the top will be frozen inside the plug before reaching the brine crown. The minimum value α^* is found by setting $V_o/V_1 = 0$ in Equation (29):

$$\alpha^* = \frac{\gamma_i}{1 + \gamma_w} \tag{31}$$

Note also the following relation between the overall change in porosity and superficial velocity across the upper leg:

$$\frac{(1 - \epsilon_1) - (1 - \epsilon_o)}{(1 - \epsilon_o)} = \alpha\frac{V_1 - V_o}{V_1} = \gamma_i - \alpha\gamma_w \tag{32}$$

Finally, let us look at the values of the characteristic lengths δ_i and δ_w over which the variations occur. First we notice the following relation between δ_i and δ_w:

$$\frac{\delta_w}{\delta_i} = \frac{c_w}{c_i}\alpha \tag{33}$$

This indicates that normally, for $\alpha << 1$, δ_w is much smaller than δ_i. Both lengths, as we can see from (14) and (23) depend on the heat transfer coefficient per unit volume U. Heat transfer rates in packed beds were given by Bird et al. (1960) and Littman et al. (1968). For the low Reynolds numbers of the flow in the upper leg, the Nusselt number based on particle diameter is practically constant and close to 2.0 (Littman et al., 1968). U can hence be expressed as a product of the heat transfer coefficient per unit area (obtained from the Nusselt number) and the surface area of the bed per unit volume (Bird et al., 1960). The characteristic lengths δ_i and δ_w under most counterwasher operating conditions come out to be of the order of the particle diameter.

CHANNELING: ITS CAUSES AND EFFECTS ON COUNTERWASHER OPERATION

Channeling is a well-known problem in ice counterwashers and one of the major obstacles to steady operation. The degree of disturbance created by channeling varies. Small, occasional channels have little effect or may cause a momentary upset in balance of pressures, from which the counterwasher usually recovers as the channels disappear with the moving plug. Large and frequent channels cause serious upsets which require complete shutdown of the counterwasher and a fresh start with a well-packed ice plug, after the cause for the channels has been removed.

The effect of channeling on counterwasher operation is illustrated in Figure 4. In the absence of channels (Figure 4*a*), the wash water flow through the upper leg is uniform, the pressure drop associated with it is linear and constant

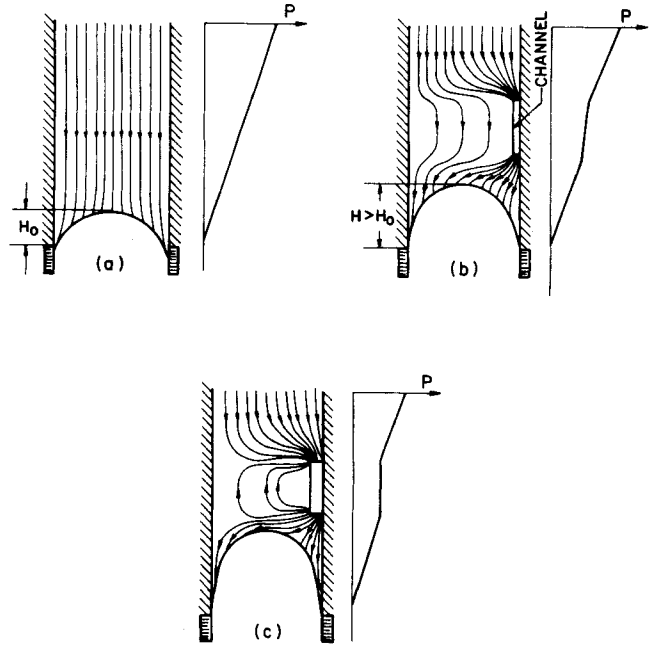

Fig. 4. Effect of channels on wash water flow and brine crown height.

(for fixed plug properties), and holds the brine crown at height H_o above the screen. When a channel opens through part of the leg (Figure 4*b*), a portion of the wash water is diverted into it. The pressure drop through this part of the leg is then reduced, which reduces the overall pressure in the upper leg and causes the brine crown to rise. The situation is still tolerable as long as the brine crown stays below the ice scraper. As soon as brine reaches the top, the counterwasher becomes ineffective.

The effect of channeling is especially harmful in pressurized counterwashers, far more than in the drained top (gravity) ones. In the latter, the upward flow of brine is counterbalanced by gravity, and the brine crown height is relatively insensitive to wash water flow. The pressurized counterwasher, however, depends on the counterflow of wash water to hold the brine crown down. Any decrease in top pressure and wash water flow through the upper leg would cause the brine to flow further up toward the ice scraper.

The split of wash water flow between the channel and the ice bed is determined by matching their respective pressure drops. In the bed we have, from Darcy's law

$$-\frac{dp}{dx} = \frac{\mu}{k}\left[\frac{Q}{A} + \epsilon w\right] \tag{34}$$

In the channel, assuming circular cross section and low Reynolds number flow, the pressure drop is given by the Poiseuille formula

$$-\frac{dp}{dx} = \frac{8\pi\mu}{a}\left(\frac{q}{a} + w\right) \tag{35}$$

where dp/dx is the pressure gradient. Setting the pressure drops equal to each other and noticing that $w << q/a$, we obtain

$$Q = \beta q - \epsilon w A \tag{36}$$

where

$$\beta = \frac{8\pi k A}{a^2} \tag{37}$$

Also, by continuity, neglecting melting and freezing, we get

$$Q + q = \alpha\left[\frac{\rho_i}{\rho_w}(1-\epsilon) w A\right] \tag{38}$$

Here the term in the square brackets is the ice production rate, and α is the wash water fraction which, with negligible melting and freezing, is equal to the wash water loss. Solving Equations (36) and (38) for q and Q, we get

$$q = wA\frac{\left[\epsilon + \alpha\frac{\rho_i}{\rho_w}(1-\epsilon)\right]}{1+\beta} \tag{39}$$

$$Q = wA\frac{\left[\beta\alpha\frac{\rho_i}{\rho_w}(1-\epsilon) - \epsilon\right]}{1+\beta} \tag{40}$$

β is a dimensionless parameter, expressing the relative flow resistances of the channel and the bed. The smaller β, the larger the portion of wash water diverted into the channel. We notice that while q is always positive, Q can become negative for very small β, even for high wash water loss. This case is illustrated in Figure 4*c*. As opposed to the narrow channel shown in Figure 4*b*, here the channel is so wide that it can hardly maintain any pressure drop along itself. The wash water in the bed next to the channel hence moves up with the plug, so that the relative velocity between the two, which gives rise to a pressure drop, is negligible. If such a channel is deep and extends below the brine crown, brine rather than wash water would flow up and reach as high as the top of the channel.

From the above discussion we conclude that two parameters control the effects of channels on the operation of the counterwasher. One is the flow resistance ratio β, which is larger for smaller channels. Clearly, higher plug permeability and larger counterwasher cross-section area make the situation better. The other is the depth or length of the channel relative to the total upper leg length and brine crown height. A short channel, even if it is wide enough to completely short-circuit the part of the upper leg through which it passes, may still leave enough of the upper leg unaffected to keep the brine crown below the ice scraper. In addition, higher wash water loss and lower porosity reduce the fraction of wash water diverted into a given channel, as can be seen from (39) and (40), but these are both undesirable.

Several causes have been observed for the opening of channels in the ice plug. Perhaps the most common one has to do with protrusions of ice on the screen, which scrape the ice plug as it moves by. The protrusions are normally formed by freezing of wash water as it comes in contact with the cold brine on the screen, or by wedging of ice crystals into the screen holes (Consie et al., 1968; Grossman, 1972). Channels created by such protrusions are easy to identify as they start from the bottom of the upper leg and are shaped as vertical grooves with constant cross section. The protrusions often detach from the screen after having created a relatively short channel. In some cases, however, the protrusion remains long enough to scrape a channel over the entire length of the upper leg, which affects washing severely.

Another common cause for channels are mechanical stresses in the plug which are normally caused by the scraper (Grossman, 1972). Cutting stresses have been observed to open cracks extending from the edge of the scraper blades down. Torsion stresses open cracks in the middle of the upper leg, typically at 45 deg. to the cutting plane (which is the plane of maximum shear). Normally, when the plug is well packed and the cutting is steady, cracks due to mechanical stresses have little tendency to develop.

The counterwasher usually tends to recover automatically from channeling as the ice plug moves up continuously and is scraped at the top. However, the channeling problem is greatly worsened by the melting action of the warm wash water. Channels in the middle or bottom of the upper leg are not affected by melting, since the wash water reaching such channels has already cooled. (We recall from our analysis of melting and freezing that the wash water reaches thermal equilibrium with the ice after flowing distance δ_w through the bed.) However, small cracks and grooves extending from the top down serve as forerunners for large channels as the wash water enters them at a temperature higher than the ice. The channels grow rapidly both in width and in depth and in many cases can never disappear. The growth rate and recovery of channels will be studied in the following section.

GROWTH OF CHANNELS IN THE UPPER LEG

Figure 5 shows a typical channel in the upper leg extending from the top down to a depth h. This channel has developed from an original forerunner (for example, crack or groove) which had opened in the plug at $t = 0$ and is shown in its present form at time t later. For simplicity, we assume the channel to have a circular cross section with a varying radius $r(x)$. The wash water entering the column at the top splits between the channel and the bed at flow rates q and Q, respectively, which vary with x due to the change in flow resistance and the added water from melt-

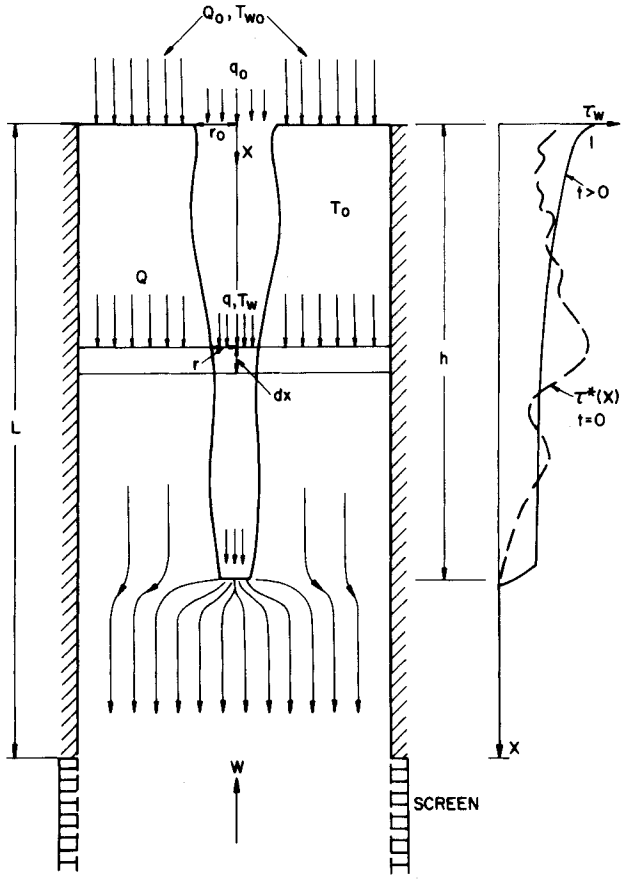

Fig. 5. Model of channel for growth rate analysis.

ing. The wash water enters the channel at a temperature $T_{wo} > T_o$, cools down as it flows along while melting some ice and increasing the channel width, then transfers the rest of its thermal energy to the ice bed at the bottom of the channel, thereby increasing its depth. Based on our previous analysis of melting and freezing, we assume both the ice and the wash water in the bed to be at the freezing point T_o, neglecting the thin melting zone of width δ_w at the top. We further assume the ice plug to have constant porosity ϵ and permeability k and to be moving up at a steady velocity w. All the flows are assumed to be one dimensional in the x direction.

Consider a control volume of thickness dx at distance x below the top, as shown in Figure 5. The channel radius, wash water temperature, and flow rate are determined as functions of x and time t by the following five equations:

(a) Continuity of ice:

$$\frac{\partial}{\partial t}[\rho_i(1-\epsilon)(A-\pi r^2)dx] = \frac{\partial}{\partial x}[\rho_i(1-\epsilon)(A-\pi r^2)w]dx - \dot{m}dx \quad (41)$$

(b) Continuity of wash water:

$$\frac{\partial}{\partial t}[\rho_w\epsilon(A-\pi r^2)dx + \rho_w\pi r^2 dx] = -\frac{\partial}{\partial x}[\rho_w(q+Q)]dx + \dot{m}dx \quad (42)$$

(c) Equilibrium of flows and pressures (see previous section):

$$-\frac{dp}{dx} = \frac{\mu}{k}\left[\frac{Q}{(A-\pi r^2)} + \epsilon w\right] = \frac{8\mu}{r^2}\left(\frac{q}{\pi r^2} + w\right) \quad (43)$$

(d) Energy balance:*

$$\frac{\partial}{\partial t}[\rho_w\epsilon\lambda(A-\pi r^2)dx + \rho_w\{\lambda + c_w(T_w - T_o)\}\pi r^2 dx] = -\frac{\partial}{\partial x}[\rho_w\lambda Q + \rho_w\{\lambda + c_w(T_w - T_o)\}q]dx \quad (44)$$

(e) Heat transfer from the water to the ice:

$$\dot{m}\{\lambda + c_w(T_w - T_o)\}dx = 2\pi r dx U'(T_w - T_o) \quad (45)$$

The flow in small and moderate size channels have low Reynolds numbers under most conditions, and the heat transfer is hence laminar with practically constant Nusselt number (Eckert, 1959):

$$Nu = \frac{2rU'}{k_w} \quad (46)$$

We define a modified heat transfer coefficient for the channel

$$\overline{U}' = \frac{\pi k_w Nu}{\rho_w c_w} \quad (47)$$

By eliminating $\dot{m}$ from Equations (41) to (45) and by introducing $\overline{U}'$ as well as the dimensionless wash water temperature τ_w and the relative heat capacity parameter γ_w [Equations (18) and (19)], we obtain the following set of simplified equations:

$$\frac{\rho_i}{\rho_w}(1-\epsilon)\left[\frac{\partial a}{\partial t} - w\frac{\partial a}{\partial x}\right] = \overline{U}'\frac{\gamma_w\tau_w}{1+\gamma_w\tau_w} \quad (48)$$

$$(1-\epsilon)\frac{\partial a}{\partial t} + \frac{\partial}{\partial x}\left[q\left(1 + \frac{8\pi kA}{a^2}\right)\right] = \overline{U}'\frac{\gamma_w\tau_w}{1+\gamma_w\tau_w} \quad (49)$$

$$\frac{\partial}{\partial t}(a\tau_w) + \frac{\partial}{\partial x}(q\tau_w) = -\overline{U}'\frac{\tau_w}{1+\gamma_w\tau_w} \quad (50)$$

where a is the channel cross-section area:

$$a = \pi r^2 \quad (51)$$

The boundary and initial conditions for the three unknowns a, τ_w, and q are

$$\text{at} \quad t = 0 \quad a = a^*(x) \quad \tau_w = \tau^*(x) \quad (52a)$$

$$\text{at} \quad x = 0 \quad \tau_w = 1 \quad q = q_o(t) \quad (52b)$$

where $a^*(x)$ and $\tau^*(x)$ describe the area and temperature distributions in the original crack as it opens, both specified initially, and $q_o(t)$ is the instantaneous wash water flow rate into the channel at the top, which depends on the pressure difference across the upper leg as well as on the channel width and depth. $q_o(t)$ hence depends on the results of the solution and will be treated as a parameter.

Equations (48), (49), and (50) are valid in the channel zone $0 < x < h(t)$. For the zone below it, where $h(t) < x < L$

$$\tau_w = 0; \quad a = 0; \quad q = 0 \quad (53)$$

Once a, τ_w, and q are determined, the bed flow rate Q and pressure drop dp/dx can be calculated from Equation (43), which can be rewritten, with small quantities neglected, as

* As in the melting and freezing analysis, the reference energy level is chosen such that ice at T_o has zero energy.

$$-\frac{dp}{dx}=\frac{\mu}{k}\left[\frac{Q}{A}+\epsilon w\right]=\frac{8\pi\mu q}{a^2} \qquad (43a)$$

The two solutions, in the channel zone and in the zone below it, are matched by matching their total flow rates.

The solution of Equations (48) to (50) is considerably simplified by making use of the fact that $\gamma_w << 1$. A comparison of orders of magnitude between the terms in the equations show the following: τ_w is of order unity, the term $8\pi kA/a^2$ [previously defined as β, Equation (37)] is of order unity for moderate size channels (which divert between 10 and 90% of the wash water from the bed) and is much smaller than unity for large channels, γ_w is typically of order 10^{-2}, $\partial a/\partial t$ and $w(\partial a/\partial x)$ are of order $\gamma_w\overline{U}'$ [from Equation (48)]. Based on this, we can neglect terms of order γ_w with respect to unity, and the following simplifications can be made: In Equation (49) the term in the square brackets can be isolated and written as the difference between the two other terms, both of order $\gamma_w\overline{U}'$. In integrating the equation with respect to x and substituting the boundary conditions, the expression resulting from this difference of terms can be neglected with respect to the others, and we obtain

$$\frac{q}{q_o}=\frac{1+8\pi kA/a_o^2}{1+8\pi kA/a^2} \qquad (54)$$

which is a relation between the channel area and flow rate expressing continuity under equilibrium of pressures between channel and bed. In Equation (50) the term on the right-hand side is of order $\overline{U}'$; the first term on the left can be written as the sum of two terms, where the first, $\tau_w(\partial a/\partial t)$, is of order $\gamma_w\overline{U}'$ and can be neglected, and the second, $a(\partial\tau_w/\partial t)$, is small except for very short times. This is illustrated by the temperature curves shown in Figure 5. At $t = 0$, the temperature distribution of the water in the channel [as given by $\tau^*(x)$] is random, whatever it happens to be when the original crack opens. Within one flow time through the channel, all the water originally there is replaced by fresh wash water coming from the top at an initial temperature $\tau_w = 1$, and the temperature distribution is then as shown qualitatively by the smooth curve in Figure 5. A situation is now reached where changes in the distribution occur at the same rate as the relative changes in a, which are of order γ_w. Equation (50) can hence be written, except for very short times, as

$$\frac{\partial}{\partial x}(q\tau_w)=-\overline{U}'\tau_w \qquad (55)$$

If the variations in flow rate along the channel are small [which is the case for channels of relatively uniform cross section area, as we can see from (54)], Equation (55) can be integrated to give the temperature distribution

$$\tau_w=\exp\left[-\frac{\overline{U}'x}{q_o}\right] \qquad (56)$$

Clearly, the higher the flow rate and the lower the heat transfer coefficient, the larger the characteristic length of the temperature variations in the channel. Calculation of the parameter inside the square brackets in (56) for many typical cases (for example, production rates of the order of 10 kg/s · m^2 and channels a few centimeters long) shows it to be a number much smaller than unity. The physical meaning of this is that the wash water looses very little of its thermal energy as it flows down the channel. Indeed, we have seen that $\partial a/\partial t$, which depends on the amount of ice melted off the sides of the channel, is of order $\gamma_w\overline{U}'$.

Finally, we can rewrite Equation (48) as

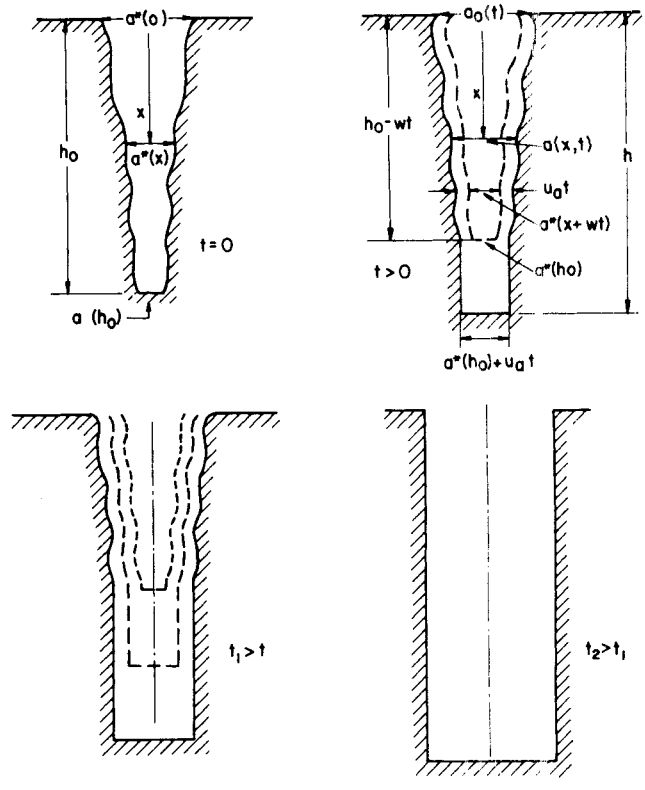

Fig. 6. Growth of channel due to melting by wash water.

$$\frac{\partial a}{\partial t}-w\frac{\partial a}{\partial x}=u_a \qquad (48)$$

where u_a represents the local melting velocity of the channel walls and is given by

$$u_a=\frac{\rho_w}{\rho_i}\gamma_w\frac{\overline{U}'\tau_w}{1-\epsilon} \qquad (57)$$

For small temperature variations in the channel, u_a is practically constant, and Equation (48a) can be integrated to give a solution for a

$$a=a^*(x+wt)+u_at \qquad (58a)$$

in the range $0 < x + wt < h_o$, and

$$a=a^*(h_o)+u_at \qquad (58b)$$

in the range $h_o - wt < x < h$. h_o is the original depth of the channel at $t = 0$.

We now have a solution for the wash water flow rate and the temperature distribution in the channel, as well as for the growth rate of the channel sideways. We still have to determine the conditions controlling the channel depth h. There is a relatively short region where the wash water redistributes in the bed as it passes from the channel zone to the one below it (see Figure 5). When this happens, the wash water which had been flowing in the channel gives up the remainder of its thermal energy, transferring it to the bed and melting some ice at the bottom of the channel. The heat transfer coefficient for this is very high, as we have seen in our previous melting and freezing analysis, and therefore all this melting occurs within a very short distance from the bottom of the channel. We can therefore write for the change in h within time dt

$$dh=(u_h-w)dt \qquad (59)$$

where w is the upward velocity of the plug and u_h is the speed at which the ice at the bottom melts. An energy balance for the melting ice (neglecting terms of order

γ_w with respect to unity) gives the following expression for u_h:

$$\rho_w c_w q(h)dt[T_w(h) - T_o] = \rho_i(1-\epsilon)\lambda a(h)u_h dt \quad (60)$$

which, when substituted in (59), yields

$$\frac{dh}{dt} = \left[\frac{\rho_w}{\rho_i}\frac{\gamma_w}{1-\epsilon}\tau_w(h)\frac{q(h)/a(h)}{w} - 1\right]w \quad (61)$$

Clearly, the growth rate of the channel in depth increases with $\tau_w(h)$. As we have seen before, in many typical cases the wash water does not cool much as it flows down the channel, and $\tau_w(h) \simeq 1$. We notice that the growth rate is proportional to γ_w as well as to the ratio between the downward wash water velocity at the bottom of the channel and the upward velocity of the plug. γ_w is a small number, and the second parameter could be fairly large; hence dh/dt can be positive, negative, or zero. Making γ_w as small as possible (that is, using wash water temperature as close to freezing as possible) would make dh/dt negative and help get rid of the channel.

Equation (61) contains in an implicit form the parameter $q_o(t)$ which is still to be specified. Once this is done, the equation can be solved for h with the initial condition $h = h_o$. The solution for the channel growth is illustrated in Figure 6, which shows a channel developing from some initial shape. The channel growth sideways is independent of the channel flow rate and is much slower than the growth in depth. The latter is opposed by the upward plug motion and depends very strongly on the flow rate. We notice that after enough time the initial channel shape is forgotten, and in the case of one-dimensional flow considered here, the channel becomes constant in cross-section area.

Our solution is now complete in terms of the wash water flow rate into the channel $q_o(t)$. This flow rate is a function of the pressure drop across the upper leg, which depends on the control system used for the counterwasher. In some cases the pressure drop is maintained fixed; in others it is coupled with the channel size as the control system keeps a constant wash water loss. For each particular case, $q_o(t)$ can be expressed in terms of the parameter being fixed through the relation between total pressure drop and channel flow rate obtained by integrating dp/dx from Equation (43a) along the upper leg. Substitution of this value of $q_o(t)$ in the results for the wash water flow rate and temperature distributions, and the growth rate sideways and in depth, will complete the solution.

ACKNOWLEDGMENT

The author wishes to express his sincere thanks to Drs. W. Gibson and D. Siegelman of AVCO Systems Division for their useful comments and suggestions on this work.

Particular thanks are due to Professor R. F. Probstein of Massachusetts Institute of Technology for his reviewing and criticism of this manuscript.

NOTATION

a = channel cross-section area
a_o = channel cross-section area at $x = 0$
a^* = channel cross-section area at $t = 0$
A = cross-section area of the plug
c_i = specific heat of ice
c_w = specific heat of water
h = channel depth
h_o = channel depth at $t = 0$
H = brine crown height
H_o = brine crown height with no channels
k = permeability
k_w = thermal conductivity of water
L = total upper leg length
$\dot{m}$ = mass of ice melted per unit volume and time
Nu = Nusselt number [Equation (46)]
p = pressure
q = wash water flow rate in the channel
q_o = wash water flow rate into the channel at $x = 0$
Q = wash water flow rate in the bed
r = channel radius
t = time
T_o = freezing temperature of fresh water
T_i = local ice temperature
T_{io} = temperature of ice emerging from brine crown at bottom of upper leg
T_w = local wash water temperature
T_{wo} = temperature of wash water entering counterwasher at top of upper leg
u_a = growth rate of the channel sideways [Equation (48a)]
u_h = growth rate of the channel in depth [Equation (60)]
U = heat transfer coefficient between water and ice in packed bed
U' = heat transfer coefficient from water to ice in the channel
$\overline{U}'$ = modified heat transfer coefficient from water to ice in the channel
v = wash water velocity
v_o = wash water velocity at $z = 0$
v_1 = wash water velocity at $y = 0$
V = wash water superficial velocity [Equation (8)]
V_o = wash water superficial velocity at $z = 0$
V_1 = wash water superficial velocity at $y = 0$
V' = wash water superficial velocity in the equilibrium zone
w = ice plug velocity
W = ice superficial velocity [Equation (9)]
W_o = ice superficial velocity at $z = 0$
W_1 = ice superficial velocityy at $y = 0$
x = coordinate along the channel (Figure 5)
y = coordinate measured from top of counterwasher downward (Figure 2)
z = coordinate measured from brine crown upward (Figure 2)

Greek Letters

α = wash water fraction [Equation (27)]
α_o = wash water loss [Equation (30)]
α^* = minimum wash water fraction [Equation (31)]
β = flow resistance ratio [Equation (37)]
γ_i = relative ice heat capacity parameter [Equation (7)]
γ_w = relative wash water heat capacity parameter [Equation (19)]
δ_i = characteristic length of freezing zone [Equation (14)]
δ_w = characteristic length of melting zone [Equation (23)]
ϵ = ice plug porosity
ϵ_o = porosity at $z = 0$
ϵ_1 = porosity at $y = 0$
ϵ' = porosity in the equilibrium zone
λ = latent heat of fusion
μ = water viscosity
ρ_i = density of ice
ρ_w = density of water
τ_i = dimensionless ice temperature [Equation (6)]
τ_w = dimensionless wash water temperature [Equation (18)]
τ^* = dimensionless temperature τ_w in the channel at $t = 0$

LITERATURE CITED

Brian, P. L. T., "Engineering for Pure Water—Part II: Freezing," *Mech. Eng.*, **90**, 42 (1968).

Barduhn, A. J., "The Freezing Process for Water Conversion in the United States," *Proceedings, First International Symposium on Water Desalination*, Washington, D.C., October 3-9, 1965, U.S Department of Interior, **2**, 641 (1967).

Bosworth, C. M., S. A. Carfagno, and D. J. Sandell, Office of Saline Water Research and Development Progress Report No. 23, U.S. Department of Interior (1959).

Bosworth, C. M., A. J. Barduhn, S. A. Carfagno, and D. J. Sandell, Office of Saline Water Research and Development Progress Report No. 32, U.S. Department of Interior (1959).

Hahn, W. J., R. C. Burns, R. S. Fullerton, and D. J. Sandell, Office of Saline Water Research and Development Progress Report No. 113, U.S. Department of Interior (1964).

Mixon, F. O., "Calculation of Liquid Flow Path in a Rectangular Wash-Separator Column with Vertical Filter Screens," Research Triangle Institute Report on OSW Contact 379 (1964).

Hahn, W. J., "Countercurrent Wash Separation Column Design," *OSW Symposium on Freezing and Ion Adsorption*, Hollywood, California, (Nov. 15-17, 1965). (Not published)

Wiegandt, H. F., Office of Saline Water Research and Development Progress Report No. 41, U.S. Department of Interior (1960).

Consie, R., D. Emmermann, J. Fraser, W. B. Johnson, and W. E. Johnson, Office of Saline Water Research and Development Progress Report No. 295, U.S. Department of Interior (1968).

Sherwood, T. K., P. L. T. Brian, A. F. Sarofim, and K. A. Smith, Office of Saline Water Research and Development Progress Report No. 436, U.S. Department of Interior (1969).

Shwartz, J., and R. F. Probstein, "An Analysis of Counterwashers for Freeze-Distillation Desalination," *Desalination*, **4**, 5 (1968).

Barak, A., and G. Dagan, "An Analytical Investigation of the Flow in the Saturated Zone of Ice Counterwashers," *AIChE J.*, **16**, 10 (1970).

Kemp, N. H., "Analytical Solution of a Sink Model of a Two-Dimensional Counterwasher," *Desalination*, **12**, 127 (1973).

Probstein, R. F., and J. Shwartz, "Method of Separating Solid Particles from a Slurry with Wash Column Separators," *U.S. Patent No. 3,587,859* (June, 1971).

Shwartz, J., and R. F. Probstein, "Experimental Study of Slurry Separators for Use in Desalination," *Desalination*, **6**, 239 (1969).

Grossman, G., "Experimental Study of Pressurized Counterwasher for Freeze-Crystallization Desalination," *OSW Symposium on Freezing*, Boston, Mass. (Sept. 20-22, 1972). (Not published)

Bird, R. B., W. E. Stewart, and E. N. Lightfoot *Transport Phenomena*, pp. 411-412, Wiley, New York (1960).

Littman, H., R. G. Barile, and A. H. Pulsifer, "Gas-Particle Heat Transfer Coefficients in Packed Beds at Low Reynolds Numbers," *Ind. Eng. Chem. Fundamentals*, **7**, 554 (1968).

Eckert, E. R. C., *Heat and Mass Transfer*, pp. 199-200, McGraw Hill, New York (1959).

Manuscript received April 29, 1976; revision received August 3, and accepted August 9, 1976.

Simulation of an Electrochemical Carbon Dioxide Concentrator

The performance of an electrochemical device for the concentration of carbon dioxide from the atmosphere of a spacecraft cabin is analyzed. The removal rates as well as the concentration distributions of the different species are calculated for any set of operating conditions by a model which embodies the fundamental electrolyte properties and design parameters.

OMAR E. ABDEL-SALAM

and

JACK WINNICK

Chemical Engineering Department
University of Missouri-Columbia
Columbia, Missouri 65201

SCOPE

Electrochemical concentration emerged in the last few years as the best technique for carbon dioxide control in a long duration manned space flight (Winnick et al., 1974). There are two different designs under development for possible applications in a life-support system (Huddleston and Aylward, 1975; Woods et al., 1975). The former design has undergone several modifications in the past few years in order to improve its efficiency and widen its capability in various environment. First, a new electrolyte (tetramethylammonium carbonate) was introduced to replace cesium carbonate. Second, a new cathode with a relatively high porosity was found to improve the carbon dioxide removal rate to a great extent. Third, the matrix material and compression were changed in order to minimize the internal cell resistance and chemical deterioration in the electrolyte medium.

Preliminary experiments showed that these changes had a significant effect on the carbon dioxide removal rate. To obtain an optimum system design it was necessary to identify the factors which determine the carbon dioxide removal rate as well as the limits of cell operation. This was done through a model which simulates the fundamental transport processes taking place in the cell.

The carbon dioxide concentration is a multistep process involving mass transport in gas phases, chemical absorption and reaction in a liquid phase, and ionic transport in an electrolyte medium. The analysis of these processes (Lin and Winnick, 1974) yields two nonlinear ordinary differential equations which can be solved to obtain the carbon dioxide removal rate as well as the concentration distribution of the different species. This model was successfully used in simulating the performance of the early designs which used Cs_2CO_3 electrolyte.

Here we examine the applicability of this model in the present situation by utilizing the new electrolyte properties and the changes associated with the new cathode and matrix designs. The model is then used in the design of a full scale unit. In addition to operating

Correspondence concerning this paper should be addressed to Jack Winnick.